

Dark matter content of ETGs and its relation to the local density of galaxies

A. Nigoche-Netro¹, G. Ramos-Larios¹, R. Díaz⁴, E. de la Fuente¹, P. Lagos⁵, A. Ruelas-Mayorga³, J. Mendez-Abreu² and S. N. Kemp¹

¹Instituto de Astronomía y Meteorología, CUCEI, Universidad de Guadalajara, Guadalajara, Jal. 44130, México
email: anigoche@gmail.com

²Instituto de Astrofísica de Canarias, Calle Vía Láctea s/n, E-38205 La Laguna, Tenerife, Spain

³Instituto de Astronomía, Universidad Nacional Autónoma de México, Cd. Universitaria, México, D.F. 04510, México

⁴Gemini Observatory, 950 N Cherry Ave, Tucson AZ, USA

⁵Instituto de Astrofísica e Ciências do Espaço, Universidade do Porto, CAUP, Rua das Estrelas, 4150-762 Porto, Portugal

Abstract. We study the behaviour of the dynamical and stellar mass inside the effective radius as function of local density for early-type galaxies (ETGs). We use several samples of ETGs - ranging from 19000 to 98000 objects - from the ninth data release of the Sloan Digital Sky Survey. We consider Newtonian dynamics, different light profiles and different initial mass functions (IMF) to calculate the dynamical and stellar mass. We assume that any difference between these two masses is due to dark matter and/or a non-universal IMF. The main results are: (i) the amount of dark matter (DM) inside ETGs depends on the environment; (ii) ETGs in low-density environments span a wider DM range than ETGs in dense environments; (iii) the amount of DM inside ETGs in the most dense environments will be less than approximately 55-65 per cent of the dynamical mass; (iv) the accurate value of this upper limit depends on the impact of the IMF on the stellar mass estimation.

Keywords. Galaxies: fundamental parameters. Galaxies: photometry, distances and redshifts. Cosmology: dark matter

1. The sample of ETGs

We use a sample of approximately 98000 ETGs from SDSS-DR9 (York *et al.* 2000) in the g and r filters. The galaxies are distributed over a redshift interval $0.0024 < z < 0.3500$. This sample will be called hereafter, the “Total-SDSS-Sample”. The selection criteria are the same we used in earlier papers (Hyde & Bernardi 2009a; Nigoche-Netro *et al.* 2010).

Selecting only ETGs from the morphological classification of the Zoospec catalogue (Lintott *et al.* 2008) and considering our selection criteria the sample is reduced to approximately 27000 ETGs. The galaxies with this added criterion have a higher probability of being ETGs. This sample shall be referred to as “Morphological-SDSS-Sample”. In addition, if we want to control possible streaming motions, redshift bias, and evolutionary effects, we have to compile a relatively nearby and volume-limited sample. The redshift range $0.04 \leq z \leq 0.08$ corresponds to a volume that fits these characteristics (Nigoche-Netro *et al.* 2008, 2009). The resulting sample contains approximately

19 000 ETGs. This sample is approximately complete for $\log(\mathbf{M}_{\text{Virial}}/\mathbf{M}_{\text{Sun}}) > 10.5$ (Nigoche-Netro *et al.* 2010, 2011). We shall refer to it as the ‘‘Homogeneous-SDSS-Sample’’.

The photometry and spectroscopy of the galaxy samples drawn from the DR9 have been corrected for different biases and are the same that we have used in previous papers (Nigoche-Netro *et al.* 2015) for full details.

2. The stellar and virial mass of the ETGs

The stellar mass. The total stellar or luminous mass was obtained considering different stellar population synthesis models, using a universal IMF (Salpeter or Kroupa) and different brightness profiles (de Vaucouleurs or Sérsic). The combination of these ingredients results in three mass estimations, as follows (Nigoche-Netro *et al.* 2015):

- de Vaucouleurs Salpeter-IMF stellar mass,
- Sérsic Salpeter-IMF stellar mass,
- Kroupa-IMF stellar mass.

The virial mass. The total virial or dynamical mass was obtained using an equation from Poveda (1958). This method assumes Newtonian mechanics and virial equilibrium for the galaxies in question. The equation is as follows:

$$\mathbf{M}_{\text{Virial}} \sim K(n) \frac{r_e \sigma_e^2}{G}, \quad (2.1)$$

where $\mathbf{M}_{\text{Virial}}$, r_e and, σ_e represent the total virial mass, the effective radius and the velocity dispersion inside r_e , respectively. G is the gravitational constant and $K(n)$ is a scale factor that depends on the Sérsic *index* (n) as follows Cappellari *et al.* (2006):

$$K(n) = 8.87 - 0.831n + 0.0241n^2, \quad (2.2)$$

The amount of mass within an effective radius corresponds to 0.42 times the total mass previously calculated. This mass may or may not be luminous.

3. Density of galaxies

The projected density of galaxies (Σ_N) was computed following the method described in Aguerri *et al.* (2009). They used the projected co-moving distance to the N th nearest neighbour (d_N) of the target galaxy as follows:

$$\Sigma_N \sim \frac{N}{\pi(d_N)^2}, \quad (3.1)$$

The local density was calculated using the third, fifth, eighth, and tenth nearest neighbours, for both the spectroscopic and photometric samples. In this work we use the local density considering the tenth nearest neighbours to avoid biases due to completeness of the SDSS survey.

4. Distribution of the difference between dynamical and stellar mass as function of local density of galaxies

From Fig. 1, we can see that the distribution of galaxies in the $\log(\mathbf{M}_{\text{Virial}}/\mathbf{M}_{\text{Sun}}) - \log(\mathbf{M}_{\text{Star}}/\mathbf{M}_{\text{Sun}})$ - density plane is similar for all samples, indicating that our results are not dependent on which galaxy sample is used or which galaxy is considered the nearest neighbour. We can see that the distribution is not random but rather has a bell-shape and that galaxies in the lowest density region cover the whole range of difference between virial and stellar mass. This range of the difference between masses decreases while the density increases. In all cases, we can see that the maximum of the density distribution is at about 0.35-0.45 in $\log(\mathbf{M}_{\text{Virial}}/\mathbf{M}_{\text{Sun}}) - \log(\mathbf{M}_{\text{Star}}/\mathbf{M}_{\text{Sun}})$. In linear values we find

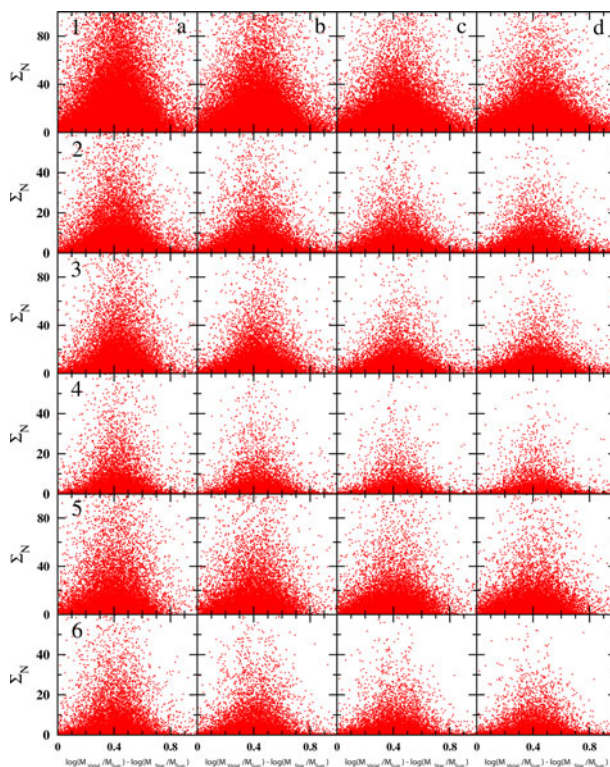


Figure 1. Distribution of the logarithmic difference between dynamical and stellar mass inside r_e as function of density of galaxies for different samples of ETGs considering a Kroupa-IMF stellar mass. Rows 1-2, 3-4 and 5-6 correspond to the total, morphological, and homogeneous SDSS samples, respectively. Rows 1, 3, and 5 are data from the photometric sample. Rows 2, 4 and 6 are data from the spectroscopic sample. Columns a, b, c, d are the data considering the third, fifth, eight, and tenth nearest neighbours respectively.

that the maximum of the density distribution has a difference between masses of about 55-65 per cent of the virial mass.

The previously discussed results were found using the Kroupa-IMF stellar mass, however we have found similar results for the de Vaucouleurs Salpeter-IMF and Sérsic Salpeter-IMF samples. There are two differences between the Kroupa and Salpeter IMF samples that do not change our general findings. The first one is that the average DM dispersion of the Sérsic-Salpeter-IMF samples ($\sigma_M \sim 0.12$) is less than the dispersion of the Kroupa IMF ($\sigma_M \sim 0.16$) and the de Vaucouleurs-Salpeter IMF ($\sigma_M \sim 0.16$) samples. This finding agrees with the one obtained by (Taylor *et al.* 2010) that find that the dynamical and stellar masses correlate best when the structure of the galaxy is taken into account. The second difference is that there is a small shift (approximately 10%) towards higher amounts of dark matter for the Salpeter IMF samples with respect to the Kroupa samples.

References

- Aguerri, J. A. L., Méndez-Abreu, J., & Corsini, E. M., 2009, *A&A*, 495, 491
 Cappellari, M., Bacon, R., Bureau, R., *et al.* 2006, *MNRAS*, 366, 1126
 Hyde, J. B. & Bernardi, M. 2009, *MNRAS*, 394, 1978
 Lintott, C. J., Schawinski, K., Slosar, A., *et al.* 2008, *MNRAS*, 389, 1179
 Nigoche-Netro, A., Ruelas-Mayorga, A., & Franco-Balderas, A. 2008, *A&A*, 491, 731

- Nigoche-Netro, A., Ruelas-Mayorga, A., & Franco-Balderas, A. 2009, *MNRAS*, 392, 1060
Nigoche-Netro, A., Aguerri, J. A. L., Lagos, P., *et al.* 2010, *A&A*, 516, 96
Nigoche-Netro, A., Aguerri, J. A. L., Lagos, P., *et al.* 2011, *A&A*, 534, 61
Nigoche-Netro, A., Ruelas-Mayorga, A., Lagos, P., *et al.* 2015, *MNRAS*, 446, 85
Poveda, A. 1958, *BOTT*, 2, 3 1
Taylor, E. N., Franx, M., Brinchmann, J., *et al.* 2010, *ApJ*, 722, 1
York, D. G., *et al.* 2000, *AJ*, 120, 1579